Oxygen Isotopic Analysis of Belemnites: Implications for Water Temperature and Life Habits in the Jurassic Sundance Sea

By

Amanda Adams

A thesis submitted in partial fulfillment of the requirements of the degree of

Bachelor of Arts
(Geology)

at

Gustavus Adolphus College

2013

Oxygen Isotopic Analysis of Belemnites: Implications for Water Temperature and Life Habits in the Jurassic Sundance Sea

By
Amanda Adams
Under the supervision of Dr. Julie Bartley

ABSTRACT

Stretching across much of the west-central United States, the Jurassic-aged (164 Ma) Sundance Formation is all that remains of the largest continental seaway in the past 250 million years. Despite its wide extent and excellent exposure, little is known about the temperature or chemistry of this ancient inland sea, making it an ideal choice for studying the geochemistry of the now dry sea. The Sundance Formation preserves a diverse array of well-preserved marine fossils, including belemnites, an extinct relative of today's squid. Analysis of oxygen isotopic composition of belemnites permits calculation of paleotemperatures for this seaway. In this study, subsamples of 36 well-preserved adult belemnites yielded average paleotemperatures of 13-17˚C for the Sundance Seaway. Comparisons between adult and juvenile belemnites also suggest that these cephalopods occupied distinct habitats during different life stages.

ACKNOWLEDGEMENTS

I would like to thank my advisor Dr. Julie Bartley as well as Dr. Laura Triplett and Dr. Jim Welsh of the Geology department at Gustavus Adolphus College for their encouragement and guidance. I would also like to thank Bill Wahl (Wyoming Dinosaur Center) for his help in formulating ideas as well as sample collection. I would like to thank Dr. David Fox and Maniko Solheid (University of Minnesota) for the use of the stable isotope laboratory facility and help in analyzing samples, and the Lee and Ginny Petersen fund for the financial support for the analysis. I would also like to thank my fellow Geology majors at Gustavus for their endless support.

TABLE OF CONTENTS

Abstract…….2

Acknowledgements……...3

Figures and Tables…….5

Introduction……...6

Geologic Setting……8

Methods……...10

Results……12

Assessment of
Diagenesis……13

Discussion……16

Conclusion……...19

References..……27

FIGURES AND TABLES

Figure/Table	Title	Page
Figure 1	Estimated boundaries of the Sundance Sea	8
Figure 2	Generalized stratigraphy of the Sundance Formation	9
Figure 3	Large-scale map of collection sites	10
Table 1	GPS coordinates of collection sites	10
Table 2 (A & B)	Summary of ICP-MS data for non-luminescent samples (A) and luminescent samples (B)	12
Table 3	$\delta^{13}C$ and $\delta^{18}O$ values by locality	13
Figure 4	Mn vs. Sr concentrations in luminescent and non-luminescent samples	14
Figure 5	Isotopic ratio comparison	14
Figure 6	Mn vs. $\delta^{18}O$ of luminescent and non-luminescent adults	15
Figure 7	Mn vs. $\delta^{18}O$ of adults and juveniles	15
Figure 8	Temperature equation comparison	16
Figure 9	Average Jurassic water temperatures	17
Appendix I	Raw ICP-MS data	21
Appendix II	Raw IR-MS data	24
Appendix III	$\delta^{18}O$ within each belemnite	26

Introduction

Paleotemperature reconstruction can be a useful tool in many fields. With modern climate shift a current major topic, it is important to map the past-climate history of the Earth in order to understand the context of the change that is occurring today and the effects it may have on the environments and ecosystems of Earth. Furthermore, a better understanding of past ecosystem conditions will help us better understand many of the extinct creatures that resided in them. This study of Jurassic belemnites provides useful paleotemperature estimates for the Sundance Sea, aiding in our understanding of past, shallow continental sea environments and adding another data point in the overall understanding of Earth's climate history.

Paleotemperature equations relate $\delta^{18}O$[1] values to ocean temperature by assuming isotopic equilibrium between calcium carbonate shell and the ambient water. This equilibrium can be affected by many factors. Part of the equilibrium is directly temperature dependent, with the partitioning of ^{18}O and ^{16}O during calcite precipitation changing as a function of temperature (Grossman, 2012). The isotopic composition is also affected by the evolution of ^{18}O:^{16}O in seawater, which is controlled indirectly by temperature, as evaporation and sequestration of water as snow and ice changes seawater isotopic composition. As ice accumulates due to lower temperatures, the ^{18}O:^{16}O ratio of seawater will increase because glacial ice stores large amounts of ^{16}O. This preference is due to the already isotopically light atmospheric moisture which then accumulates as snow, enriching the glacier with ^{16}O (Stanley, 2009). The combined effect of these two processes is that $\delta^{18}O$ increases with decreasing temperature, so low $\delta^{18}O$ values in fossil carbonates indicates warmer paleotemperatures (Henderson and Price, 2011; Ivany and Runnegar, 2010).

[1] $\delta^{18}O$ is the measure of the ratio of stable isotopes ^{18}O:^{16}O, relative to a standard, and is expressed in parts per thousand, or permil, ‰ (Pearson, 2012)

Paleothermometry can also be used to learn more about the life-habit of extinct species. Oceans are stratified, with warmer waters above the thermocline and cooler waters below the thermocline. A study by Rexfort and Mutterlose (2006) used oxygen isotope paleothermometry to reveal a general trend that modern cuttlefish inhabit warmer, shallower water when younger, then travel down past the thermocline into cooler waters as adults. Differences in $\delta^{18}O$ values between fossilized adult and juvenile belemnites may indicate the same migratory behavior in extinct coleoids that modern cuttlefish exhibit.

Belemnites are a group of extinct coleoid cephalopods, and like modern squids, possessed a soft-tissue outer body surrounding a hard internal carbonate shell called a guard (Dutton, 2007). Belemnites have been a useful tool to biostratigraphers since the early 1800s because of their wide geographical range, limited stratigraphic range (early Jurassic through end Cretaceous), and their distribution across facies, not to mention their sheer abundance (Doyle and Bennett, 1995). In the mid-1900s, belemnites began to be used for paleothermometry (Dutton, 2007) because their fossilized guards resist diagenesis and are generally secreted in oxygen isotopic equilibrium with the surrounding water as they grow (Grossman, 2012).

Several paleotemperature studies use belemnite oxygen isotopic data to determine paleotemperature (Dera, 2009; Dutton, 2007; Rosales, 2004; Stevens and Clayton, 1971). The reliability of belemnites as paleothermometers is supported by oxygen isotope studies of modern animals that secrete their shells in the same manner as belemnites, such as cuttlefish and oysters, where temperatures calculated from $\delta^{18}O$ values from collected shells are within a few degrees of actual recorded water temperatures (Rexfort and Mutterlose, 2006; Ullman, 2010). Most paleotemperature reconstruction studies have focused on open ocean environments; in contrast,

few data exist for continental seaways and only preliminary work has been done for the Sundance Sea (Ploynoi, 2007).

The Sundance Sea is the largest North American continental seaway in the past 250 million years, comprising four episodes of transgression. Of interest in this study is the transgression taking place during the Oxfordian through early Kimmeridgian stages (164-152 million years ago; Imlay, 1947; USGS, 2005). During this time a layer of gray-green shale interbedded with sandstone, now referred to as the Sundance Formation, was deposited (Imlay, 1947) as far east as the Dakotas and southward to New Mexico (Stanley, 2009).

Little is documented of the paleotemperature or geochemistry of this ancient inland sea, making it an ideal choice for geochemical study. This study will use oxygen isotopic composition of well-preserved adult belemnites from the Bighorn Basin of northern Wyoming to calculate paleotemperatures of this widespread Jurassic North American seaway and provide preliminary data about the differences in paleodepth habitats during different life stages for belemnites.

Geologic Setting

During the Jurassic rapid sea floor spreading created shallow ocean basins, resulting in global sea level rise (Kuehn, 2006). This caused the waters of the Pacific Ocean to spread out over what is now North America. One such incursion resulted in the Sundance Sea, an inland seaway reaching as far east as the Dakotas and southward to New Mexico (Figure 1; Stanley, 2009). Lasting from the

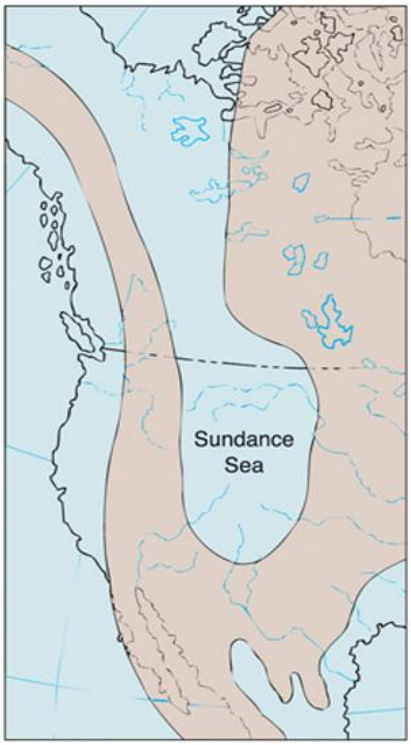

Figure 1. Estimated boundaries of the Sundance Sea (Gore, P.J.W.)

Oxfordian through early Kimmeridgian Stage (Turner, 2004) this sea deposited the mainly siliciclastic Sundance Formation. Mountain building to the west caused increased rates of sediment supply to the basin, resulting in regional regression and depositing a stratigraphic succession from deeper water shales to shallower water sandstones (Figure 2). Eventually the area filled with enough sediment and what was once an inland sea evolved to a mainly fluvial and terrestrial environment.

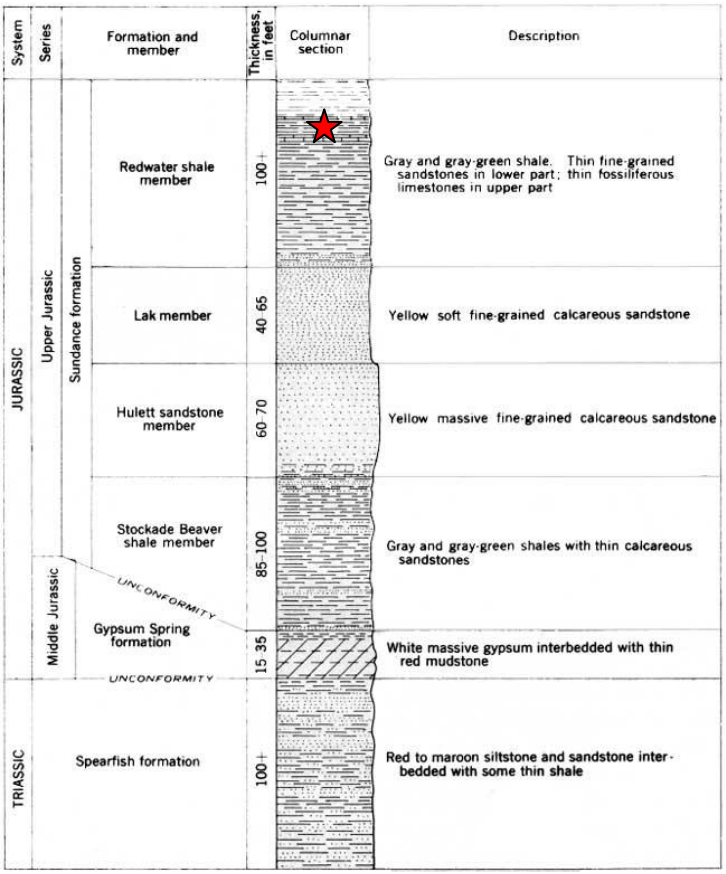

Figure 2. Generalized stratigraphic column of the Sundance Formation and its division into Members (USGS, 2005). Star indicates presence of belemnites

The Sundance Formation is divided into four members (Figure 2) that include shales, siltstones, sandstones, and limestones. The youngest member, the Redwater Shale Member, is the most important for this study, as it contains the belemnite-bearing fossiliferous layers (Imlay, 1947). Consisting primarily of gray-green shale, this member is 30 to almost 60 meters thick. Yellow sandstones and limestones are also interbedded within the shale. It is these limestones, varying in thickness from a few centimeters to several meters, which contain the marine fossils essential to this project (USGS, 2005).

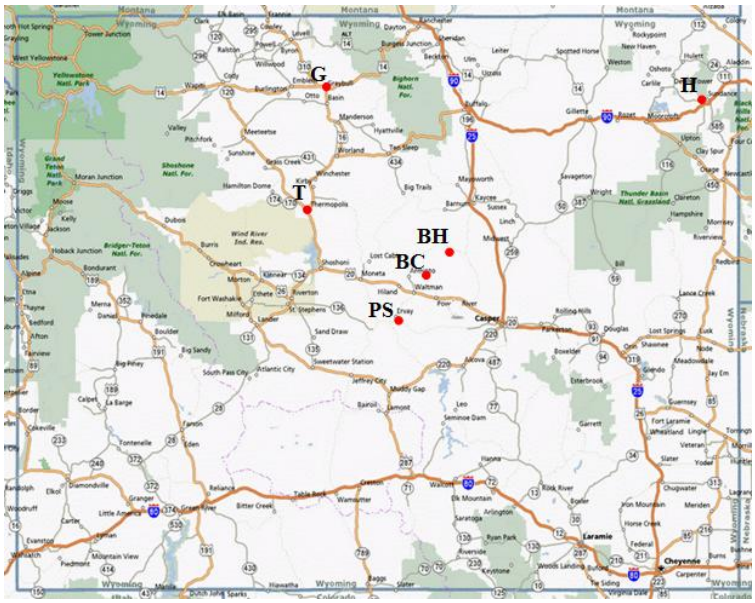

Figure 3. Approximate location of sampling localities

Thermopolis	43°37'4.53"N, 108°11'24.65"W
Greybull	44°27'50.94"N, 107°49'1.68"W
Poison Spider	42°52'55.83"N, 107°24'21.76"W
Baker's Cabin	43°10'44.53"N, 107°14'37.12"W
Belemnite Hill	43°22'35.53"N, 106°49'24.16"W
Highway	44°19'53.63"N, 104°29'34.30"W

Table 1. GPS coordinates of collection localities. Values for Baker's Cabin and Belemnite Hill are approximations

Methods

Six collection sites (Figure 3, Table 1) were chosen based on accessibility and belemnite abundance. From east to west these are labeled as Thermopolis (T), Greybull (G), Poison Spider (PS), Baker's Cabin (BC), Belemnite Hill (BH), and Highway (H) throughout the paper. All belemnites were collected from fossil concentrations weathered from outcrop, and selected for large length and width, as well as little external erosion. Six belemnites from each locality were selected for analysis, for a total of 36 adult belemnite samples. Juveniles were collected from sites T, BC, and BH by sifting ant-hills (ants carry larger objects such as small belemnites and shell fragments to the outer layer of their anthill). Three juveniles were chosen from each of the three sites for a total of 9 samples.

Each adult sample was cut longitudinally with both halves labeled. Once cut, the samples were polished with progressively finer grit sizes to prepare them for cathodoluminescence (CL) analysis. CL identifies trace elements called activators and quenchers which can be used to identify regions that have undergone diagenesis. The main activator (indicator of alteration) for

calcite is manganese and appears under CL analysis as luminescent orange, while the main quencher is ferric iron, which shows up as dark, non-luminescent areas within the fossil (O'Neill et al., 2003). Using CL, 2-3 areas with low to no luminescence were identified for drilling. Following this step, a 1mm drill bit was used to collect 1-2 mg of sample from each marked area. The juvenile belemnites were etched with acid to remove the outermost layer and then ground to a fine powder. After all sampling was complete there were a total of 87 samples.

The first step in analysis was to randomize sample order and analyze all 87 samples with the Finnigan MAT 252 isotope ratio mass spectrometer (IR-MS) located at the University of Minnesota in order to obtain $\delta^{18}O$ and $\delta^{13}C$ data. Next these samples were analyzed for major and trace element concentrations using the inductively coupled plasma mass spectrometer (ICP-MS) located at Gustavus Adolphus College. Approximately 0.5 mg of sample was dissolved in 5 ml of 2% HNO_3 spiked with an internal standard with known amounts of Be, Bi, Ga, In, Sc, and Tb. Concentrations of Fe, Mg, Mn, Ca, and Sr were measured and used to evaluate the degree of diagenesis and the potential reliability of isotopic data.

The final step in analysis was to calculate water temperature based on the isotopic signatures from each sample using the following equation from Friedman and O'Neil (1977):

$$1000ln\alpha = 2.78(10^6T^{-2}) - 2.89$$

where α is the equilibrium fractionation factor between calcite and water and T is the temperature in degrees Kelvin. In this case, α was calculated using the observed difference between the measured $\delta^{18}O$ from each sample and an assumed seawater $\delta^{18}O$ value of -1.0‰ (ice-free world; Grossman, 2012).

Results

All belemnite specimens were tested for diagenesis using cathodoluminescence (CL), trace element composition, and correlation among elemental and isotopic compositions. Observations made under CL showed high luminosity in growth bands of all belemites, as well as around the outside edge and inside the phragmacone when present. Highly luminescent areas were avoided during drilling with the exception of samples 9C, 13C, and 31C which were drilled for comparison to non-luminescent samples.

All relevent data collected from the inductively coupled plasma mass spectrometer (ICP-MS) are reported in Appendix I. Luminescent and non-luminescent samples had distinct elemental profiles (Table 2). The average Mg concentration was higher in luminescent samples

Element	Number of Samples	Average (ppm)	Standard Deviation
Mg	84	593	283.7
Mn	84	3	4.4
Fe	84	14	28.5
Sr	84	282	44.7

Table 2A. Summary of ICP-MS data for all non-luminescent samples

Element	Number of Samples	Average (ppm)	Standard Deviation
Mg	3	612	626.5
Mn	3	189	189.9
Fe	3	767	888.1
Sr	3	805	712.8

Table 2B. Summary of ICP-MS data for all luminescent samples

(612 ppm) than in non-luminescent samples (593 ppm). Luminescent samples also had higher concentrations that non-luminescent samples for Mn (189ppm vs. 3ppm, respectively), Fe (767 ppm vs. 14 ppm), and Sr (805 ppm vs. 282 ppm).

Locality	$\delta^{13}C$ VPDB (‰)	$\delta^{18}O$ VPDB (‰)
Thermopolis	2.48	-1.04
Greybull	3.51	-0.44
Poison Spider	2.41	-1.31
Baker's Cabin	2.98	-0.87
Belemnite Hill	3.76	-0.79
Highway	2.80	-0.77
Juveniles	2.60	-1.76
Luminescent	-0.57	-11.89

Table 3. Average $\delta^{13}C$ and $\delta^{18}O$ values calculated from non-luminescent samples separated by locality (listed West to East). Average values for juveniles and luminescent samples are also reported. All values are given in Vienna Pee Dee Belemnite (VPDB) ‰.

Stable isotope compositions were measured and complete data are reported in Appendix II. Average $\delta^{13}C$ values for non-luminescent adult samples across all sites were similar (avg = +3.0 ‰, n = 6, σ = 0.6). There were no distinct trends in either the N-S direction or E-W direction. Average $\delta^{18}O$ values for non-luminescent samples across all sites were also similar (avg = -0.9 ‰, n = 6, σ = 0.3). Juvenile samples from all sites sampled showed consistent results as well for $\delta^{13}C$ (avg = +2.6 ‰, n = 9, σ = 0.6) and $\delta^{18}O$ (avg = -1.8 ‰, n = 9, σ = 0.8). Luminescent samples showed lower $\delta^{13}C$ (avg = -0.6 ‰, n = 3, σ = 1.2) and $\delta^{18}O$ (avg = -11.9 ‰, n = 3, σ = 3.1) (Table 3).

Assessment of Diagenesis

The trace element compostion and the correlation between elemental and isotopic data was examined for all samples to assess diagenesis. A comparison of Mn and Sr concentrations reveals that non-luminescent samples cluster on the Sr axis with very low Mn concentrations, indicating that they are well-preserved carbonates (Figure 4). Note the two highly luminescent values shown are high in Mn, characteristic of having undergone some degree of diagenesis (Bartley et al., 2001).

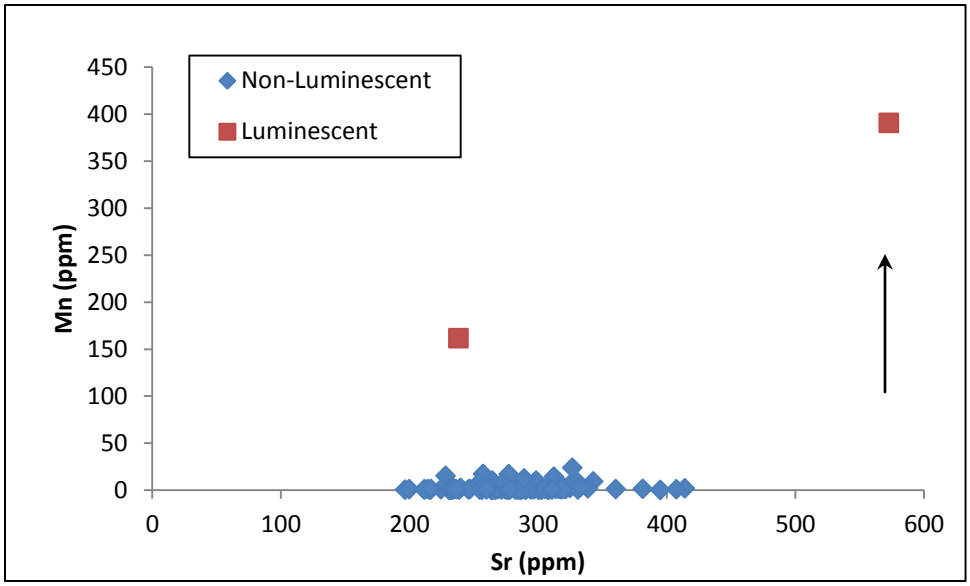

Figure 4. Mn concentration (ppm) vs. Sr concentration (ppm) in luminescent and non-luminescent samples. One data point outlier has been removed for easier interpretation (Sr: 1605, Mn: 13). Arrow indicates direction of increased likelihood of diagenesis.

Furthermore, a comparison of $\delta^{13}C$ and $\delta^{18}O$ shows the sample concentrations of $\delta^{18}O$ for all non-luminescent samples fall within a narrow range (minimum -3.3‰, maximum 0.9‰) but vary greatly with respect to $\delta^{13}C$ (minimum -0.1‰, maximum 5.3‰) (Figure 5). Typical diagenesis plots show co-variation in $\delta^{13}C$ and $\delta^{18}O$, as exhibited by the three luminescent samples in Figure 4 (Dutton, 2007). This is further evidence that all samples (not including luminescent controls) retain their original geochemistry.

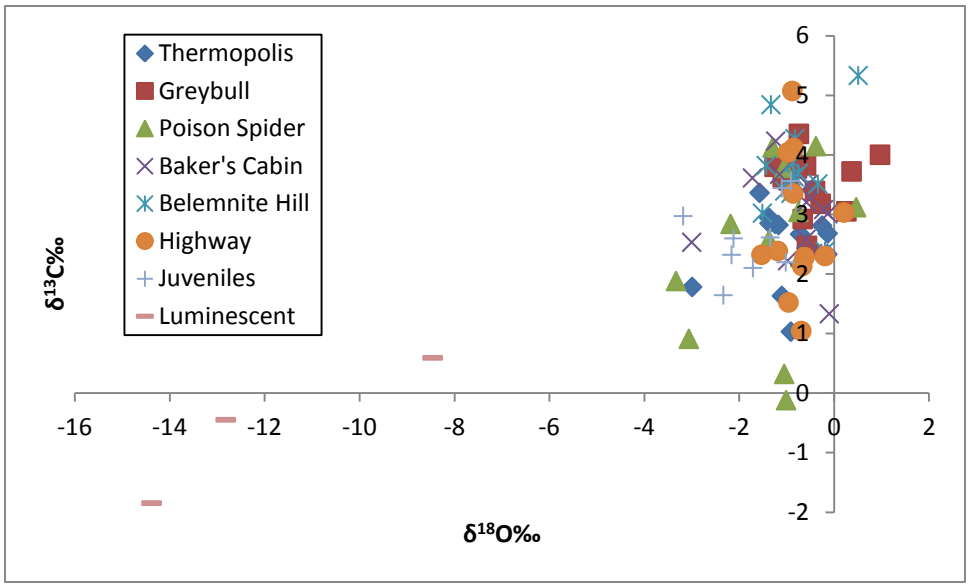

Figure 5. $\delta^{18}O$ vs. $\delta^{13}C$ of all samples separated by locality (listed in West to East). Juveniles plot within Adult non-luminescent data. All data is in VPDB ‰. Likelihood of diagenesis is greater as $\delta^{18}O$ varies with respect to $\delta^{13}C$.

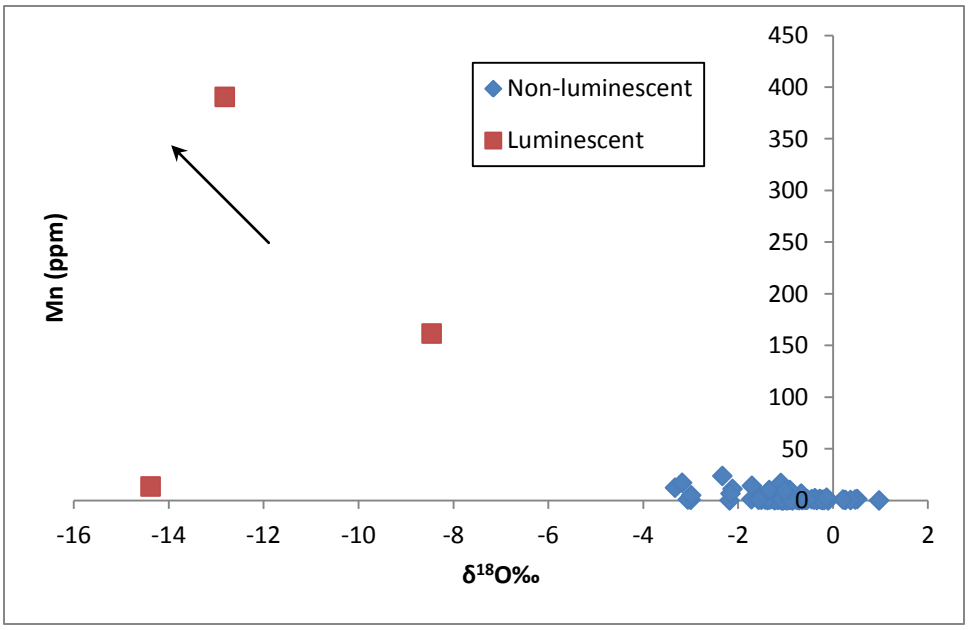

Figure 6. Mn concentration (ppm) vs. δ18O VPDB ‰ of both luminescent and non-luminescent samples. Arrow indicates direction of increased likelihood of diagenesis.

Lastly, $\delta^{18}O$ values are compared to values of Mn in Figures 6 and 7. As seen in Figure 6 all non-luminescent samples cluster within a narrow range of Mn concentration (minimum 0.2 ppm, maximum 23.9 ppm), while the three luminescent samples show greater variation in both Mn and $\delta^{18}O$. Figure 7 compares Mn concentrations to $\delta^{18}O$ values without the luminescent samples. The ratio of Mn to $\delta^{18}O$ show clustering of all adult non-luminescent samples along the x-axis. Juvenile belemnites have Mn concentrations much higher with respect to

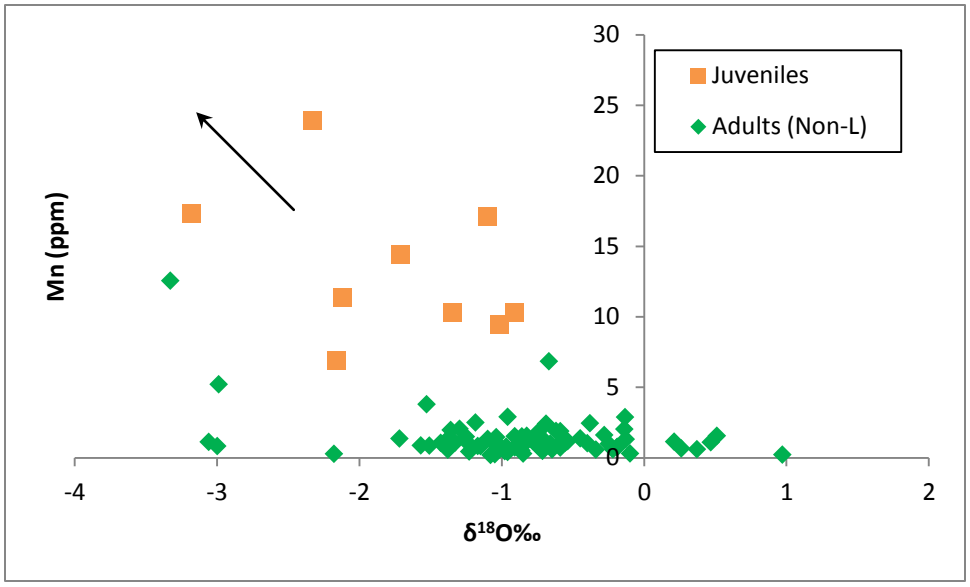

Figure 7. Mn concentration (ppm) vs. $\delta^{18}O$ VPDB ‰ of only juveniles and non-luminescent adults. Arrow indicates direction of increased likelihood of diagenesis.

$\delta^{18}O$. Typical diagenesis trends in carbonates show increasing Mn concentration with respect to $\delta^{18}O$ (Dutton, 2007), indicating that all non-luminescent samples retain their primary geochemical signals and are therefore viable candidates for paleothermometry analysis.

Discussion

All non-luminescent adult samples represent unaltered carbonates and therefore retain the original geochemistry of the ocean water. Based on these results, an average water temperature of 13-17˚C is calculated for the Sundance Sea. All conclusions are based on the assumption that belemnite calcite was secreted year-round. Appendix III shows the $\delta^{18}O$ values across each belemnite in order to determine whether there were any trends in temperature from the interior to the exterior of each belemnite. As there are no visible trends across all belemnites each sample from every belemnite was treated as a separate data point when calculating paleotemperature.

Paleotemperature was initially calculated using three different equations, each associated with paleotemperatures for distinct time periods (Paleogene: Erez and Luz, 1983; Cretaceous: Kim and O'Neil, 1997; Jurassic: Friedman and O'Neil, 1977). Each calculation was made with the assumption that the average $\delta^{18}O$ value for seawater was -1.0‰ for an ice-free world (Grossman, 2012). The

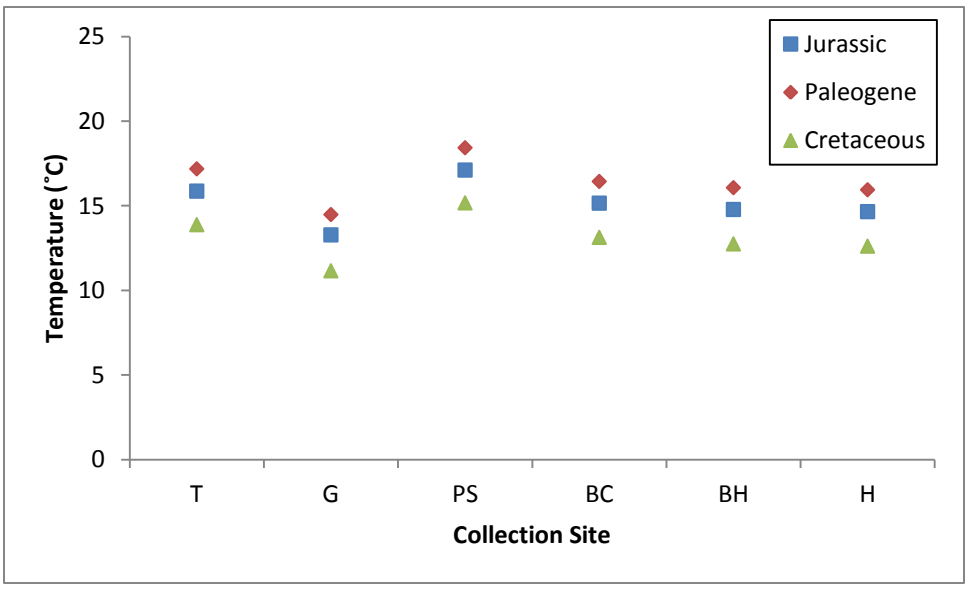

Figure 8. Average temperatures from each collection site as calculated by Jurassic, Paleogene, and Cretaceous paleotemperature equations.

average temperatures from each locality are plotted in Figure 8. For the purposes of this study conclusions will be based on those temperatures calculated from the Friedman and O'Neil (1977) equation as they were also applied to Jurassic carbonates.

A one-way ANOVA indicates that there are no statistically significant differences in mean temperature among localities ($p = 0.098$), suggesting that all adults sampled are living within the same temperature zone. Figure 9 plots average water temperatures with standard error calculated using the Jurassic paleotemperature equation (Friedman and O'Neil, 1977). Juveniles collected from Baker's Cabin (BC), Belemnite Hill (BH), and Thermopolis (T) were compared to the set of adults from the corresponding localities in a series of two-group comparison t-tests. It was found that the average temperature from the juvenile belemnites was higher for each site than that calculated for the adults; however, only sites BC and T showed statistically significant differences ($p = 0.044$, $p = 0.023$ respectively). The t-test for BH did not show a statistically significant difference between the mean temperatures of adults and juveniles ($p = 0.360$). It should be noted that the higher levels of manganese seen in the juvenile samples (Figure 7)

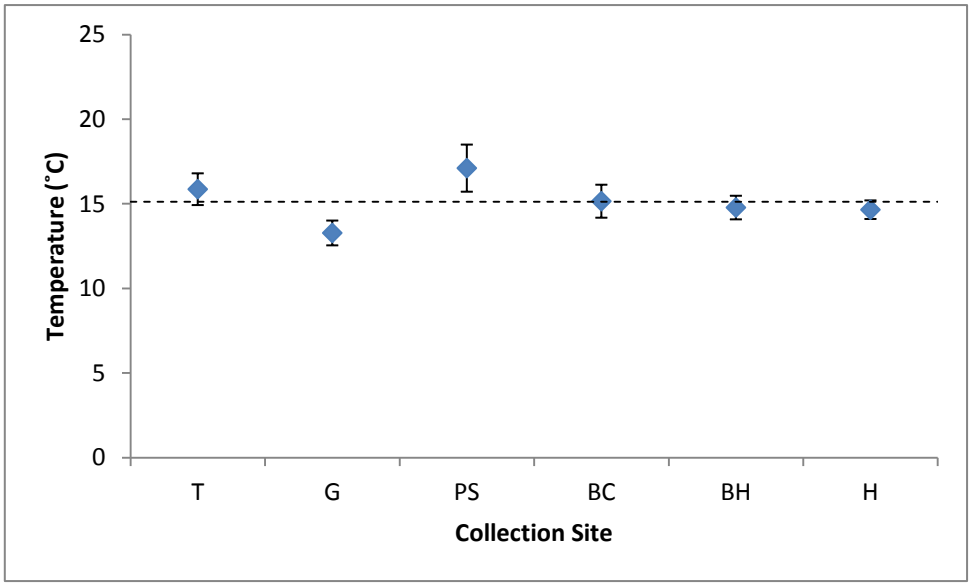

Figure 9. Average water temperature in degrees Celsius for each collection site. Collection sites are listed (from left to right) in West to East order. Data was calculated with Friedman and O'Neil paleotemperature equation. Standard error shown. Dotted line represents the running mean (15.1°C)

indicate a possibility of diagenesis. If this is the case, the higher temperature seen in the juveniles may be a result of altered $\delta^{18}O$ levels.

Because the mean temperature differences between localities can be attributed to the random nature of sample collection, the data will be considered a range for overall paleotemperature. Thus, the range of average water temperature below the thermocline for the Sundance Sea during the Late Jurassic (Oxfordian through early Kimmeridgian) is calculated as 13-17˚C, while the juvenile data gives a slightly warmer range of 16-20˚C for waters above the thermocline. Variation in temperature may be due to vertical or horizontal migration within the water column where the secreting shell would be exposed to varying environmental conditions.

These findings are similar to results obtained from a preliminary study on the Sundance Sea done with microbial buildups and belemnites (15-17˚C) from the Bighorn Basin of Wyoming (Ploynoi, 2002), a study done by Stevens and Clayton (1971) where Jurassic belemnites analyzed from New Zealand (17.6-20.5˚C), and a third study by Rosales et al. (2004) where Jurassic belemnites from Spain produced an average water temperature of 16.5˚C. These temperatures would be consistent with adults living in shallow, warmer waters like that presented by the Sundance Sea.

It is important to note that the calculated temperatures reported here may be skewed due to the environmental conditions presented by the Sundance Sea. As an epicontinental sea, the area may have been highly affected by evaporation, freshwater river input, or a combination of the two (Grossman, 2012). If evaporation played a key role in determining the ratio of ^{18}O:^{16}O in the ocean water, then the overall $\delta^{18}O$ signal of local seawater would be shifted positive, resulting in a calculated temperature lower than the actual paleotemperature. If river input plays

a major role, $\delta^{18}O$ would have shifted negative, producing a higher apparent temperature. Further investigation into the specific depositional environment and a comparison of isotopic values across many taxa should be conducted to determine to what degree these factors are playing a role in the fractionation of oxygen isotopes.

Due to the lack of well-preserved juvenile $\delta^{18}O$ data a comprehensive assessment of adult versus juvenile temperatures cannot be performed. Of the preliminary data collected, the difference in geochemical signatures suggests that juveniles inhabit warmer waters than adults. This result is similar to the findings of Wierzbowski et al. (2009) where there is a distinct change is temperature from the interior of the adult belemnite towards the outer regions. Wierzbowski et al. suggest this may be a result of change in habitat during their ontogenetic development, a characteristic common in modern squids and cuttlefish (Price et al., 2009; Rexfort and Mutterlose, 2006). Further analysis of the geochemistry of juveniles from multiple collection sites would help in making a more comprehensive conclusion on this subject.

Conclusion

Elemental analysis of non-luminescent samples from adult belemnites collected throughout the Sundance Formation of northern Wyoming show these fossils to be well preserved and therefore viable for paleothermometry tests. Average $\delta^{18}O$ values throughout all adult collection sites give a temperature range of 13-17˚C below the thermocline. A comparison between adults and juveniles show a tendency towards warmer recorded temperatures (16-20˚C) for juveniles, suggesting they are living in warmer waters above the thermocline, similar to modern squids and cuttlefish (Price et al., 2009; Rexfort and Mutterlose, 2006).

While data presented here suggest juvenile belemnites inhabit warmer waters than adults, it will be important to collect a larger sample size from a wider set of localities in order to determine with further certainty whether the difference in average water temperature is typical or if the results found here are a result of too small a sample size. Furthermore, more precise sampling techniques will be required to avoid sampling the diagenetically altered outer edge of the juveniles.

Appendix I

Sample	Locality	Mg (ppm)	Ca (ppm)	Mn (ppm)	Fe (ppm)	Sr (ppm)
01A	BC	497.92	135059	1.17	3.89	321.26
01B	BC	554.47	129009	1.07	4.57	296.83
02A	BC	1245.90	141225	1.88	8.03	278.16
02B	BC	399.27	127738	1.37	2.73	293.84
02C	BC	507.40	120557	0.59	2.76	284.94
03A	BC	455.23	116591	1.36	6.38	287.32
03B	BC	320.35	117129	1.31	5.61	214.23
04A	BC	766.21	116759	0.46	5.44	302.68
04A-D	BC	719.60	109273	0.36	6.72	286.87
04B	BC	262.93	107728	0.30	5.74	215.98
05A	BC	708.17	108064	0.82	4.71	282.07
05B	BC	249.51	92206	0.59	3.69	196.59
06A	BC	751.23	118251	0.82	1.88	259.87
06B	BC	724.98	125175	0.44	2.29	277.82
07A	BH	784.44	147056	1.05	7.54	407.50
07B	BH	355.45	91748	1.46	1.46	230.45
08A	BH	522.42	122870	1.55	8.25	315.82
08B	BH	583.36	133265	1.52	6.11	313.50
09A	BH	652.85	122368	1.77	6.38	278.18
09B	BH	336.62	103193	1.55	3.14	254.77
09C*	BH	552.22	118995	390.71	527.21	572.69
10A	BH	703.19	117378	1.06	11.04	317.85
10B	BH	401.10	134131	1.00	8.67	284.36
11A	BH	401.28	107858	0.57	3.36	238.50
11B	BH	416.79	125683	0.76	1.84	263.34
11B-D	BH	436.41	127451	0.80	2.56	271.39
12A	BH	430.77	110506	0.86	3.40	245.88
12B	BH	488.00	114378	0.51	3.62	266.63
13A	PS	571.86	140914	2.44	3.17	324.75
13A-D	PS	500.24	124012	2.07	2.75	272.22
13B	PS	1075.08	161074	2.05	6.04	414.08
13C*	PS	17.16	28807	13.72	23.53	1605.45
14A	PS	416.25	122635	0.78	3.36	294.67
14B	PS	363.19	127666	1.01	4.42	307.68
15A	PS	422.33	123257	0.25	2.21	308.11
15B	PS	458.08	103437	0.27	1.35	232.80
16A	PS	438.65	110353	0.88	5.39	231.94
16B	PS	456.68	138010	1.43	8.31	305.14
17A	PS	530.85	113906	1.31	4.59	246.94

Sample	Locality	Mg (ppm)	Ca (ppm)	Mn (ppm)	Fe (ppm)	Sr (ppm)
17B	PS	610.65	103345	1.12	8.11	199.79
18A	PS	1938.96	124782	12.55	36.88	289.16
18B	PS	440.19	116411	1.09	3.09	267.49
19A	G	526.04	160554	1.61	5.77	316.15
19B	G	636.44	126011	1.49	4.76	300.53
20A	G	379.68	125039	0.22	4.80	230.94
20B	G	429.90	120263	0.19	3.04	264.29
21A	G	441.88	117204	1.18	7.65	274.07
21B	G	422.95	127279	0.72	3.76	290.02
22A	G	421.03	125651	0.40	7.80	275.93
22B	G	639.46	135179	1.14	8.48	307.56
23A	G	286.20	111828	0.66	3.66	211.57
23B	G	733.43	121098	0.60	4.25	254.66
23C	G	359.52	102741	1.03	3.03	211.55
24A	G	441.75	108863	1.00	2.68	234.21
24A-D	G	433.17	105952	0.99	3.09	230.94
24B	G	421.67	112041	1.17	3.32	236.09
25A	H	547.98	153952	1.22	9.83	360.36
25B	H	690.81	163708	0.29	5.72	395.00
26A	H	790.38	133464	0.78	2.74	330.93
26B	H	929.12	159700	1.51	4.25	381.39
27A	H	1094.45	124759	2.41	10.56	289.48
27B	H	1366.75	130736	2.90	12.03	270.28
27B-D	H	1357.98	131041	2.95	10.18	262.89
28A	H	545.83	129844	0.75	2.45	290.49
28B	H	878.63	141724	1.14	4.94	318.74
29A	H	630.23	114450	2.49	4.16	239.76
29B	H	1375.77	118363	3.79	8.74	333.16
30A	H	1007.48	104189	1.90	3.52	256.36
30B	H	1061.87	135197	6.84	11.11	271.86
31A	T	680.39	123404	5.21	177.71	318.26
31B	T	430.99	133968	0.49	7.78	300.53
31C*	T	1265.89	92222	161.72	1750.43	238.05
32A	T	273.04	120186	0.83	4.22	283.19
32B	T	336.71	100872	0.57	4.06	256.40
32C	T	222.39	118327	0.98	2.34	224.46
32C-D	T	213.61	117283	0.97	1.77	232.80
33A	T	277.30	106360	2.03	5.66	234.40
33B	T	270.55	129211	2.88	6.40	277.06
34A	T	465.63	124650	1.06	3.52	265.39
34B	T	590.35	140373	1.96	13.92	338.75
35A	T	689.69	115436	1.33	11.21	216.74

Sample	Locality	Mg (ppm)	Ca (ppm)	Mn (ppm)	Fe (ppm)	Sr (ppm)
35B	T	768.48	133248	0.73	12.36	310.68
36A	T	423.86	113535	1.17	39.07	268.59
36B	T	558.93	123439	0.87	12.82	286.22
J1	BH	551.57	136349	10.30	33.47	298.48
J2	BH	468.68	118881	10.28	22.49	264.36
J2-D	BH	484.19	119319	9.58	21.48	279.45
J3	BH	623.77	135182	17.12	42.78	277.17
J4	BC	791.74	131052	11.37	43.02	328.62
J5	BC	604.18	101900	6.90	35.13	253.44
J6	BC	776.91	125864	14.41	55.12	312.31
J7	T	519.93	111027	17.31	161.32	257.18
J7-D	T	472.19	102926	15.34	146.42	228.07
J8	T	667.81	135745	23.90	101.83	326.59
J9	T	516.64	150663	9.41	28.28	342.89

Appendix I. Data from ICP-MS, each value is ppm of each element in the rock sample. Localities: Baker's Cabin (BC), Belemnite Hill (BH), Poison Spider (PS), Greybull (G), Highway (H), and Thermopolis (T). Calcium values are rounded to the nearest whole number. Samples labeled with D are duplicates run for reproducibility. Samples labeled with * were intentionally drilled in highly luminescent regions.

Appendix II

Sample	Locality	$\delta^{13}C$‰ VPDB	$\delta^{18}O$‰ VPDB
01A	BC	3.2	-0.58
01B	BC	3.50	-0.55
02A	BC	2.58	-0.59
02B	BC	2.34	-0.45
02C	BC	3.08	-0.22
03A	BC	3.61	-1.72
03B	BC	3.01	-0.13
04A	BC	2.22	-0.98
04B	BC	1.33	-0.1
05A	BC	2.53	-3
05B	BC	3.40	-0.65
06A	BC	3.67	-1.15
06B	BC	4.23	-1.23
07A	BH	3.82	-1.43
07B	BH	3.39	-1.04
08A	BH	4.27	-0.83
08B	BH	3.35	-0.91
09A	BH	3.69	-0.75
09B	BH	5.33	0.51
10A	BH	4.84	-1.33
10B	BH	3.63	-0.84
11A	BH	3.51	-0.34
11B	BH	2.38	-0.19
12A	BH	3.02	-1.51
12B	BH	3.87	-0.86
13A	PS	4.14	-0.38
13B	PS	4.12	-1.30
14A	PS	-0.12	-1.01
14B	PS	0.32	-1.05
15A	PS	3.78	-1.05
15B	PS	2.84	-2.18
16A	PS	3.04	-0.75
16B	PS	2.57	-1.37
17A	PS	2.28	-0.71
17B	PS	0.91	-3.06
18A	PS	1.88	-3.33
18B	PS	3.12	0.47
19A	G	3.18	-0.28
19B	G	3.80	-1.25
20A	G	4	0.97
20B	G	3.62	-1.08
21A	G	4.35	-0.74
21B	G	3.82	-0.59

Sample	Locality	$\delta^{13}C‰$ VPDB	$\delta^{18}O‰$ VPDB
22A	G	3.57	-0.96
22B	G	3.77	-0.78
23A	G	3.05	0.26
23B	G	3.72	0.37
23C	G	3.39	-0.40
24A	G	2.92	-0.66
24B	G	2.47	-0.57
25A	H	5.07	-0.88
25B	H	4.11	-0.85
26A	H	4.04	-0.97
26B	H	3.35	-0.86
27A	H	1.04	-0.69
27B	H	1.52	-0.96
28A	H	2.3	-0.19
28B	H	3.03	0.21
29A	H	2.38	-1.19
29B	H	2.32	-1.53
30A	H	2.28	-0.62
30B	H	2.13	-0.67
31A	T	1.78	-2.99
31B	T	2.67	-0.71
32A	T	2.82	-1.17
32B	T	2.95	-1.38
32C	T	2.81	-0.25
33A	T	2.33	-0.14
33B	T	2.68	-0.14
34A	T	2.84	-1.24
34B	T	2.85	-1.36
35A	T	1.63	-1.1
35B	T	1.03	-0.91
36A	T	2.47	-0.54
36B	T	3.36	-1.57
J1	BH	2.61	-1.34
J2	BH	3.56	-0.91
J3	BH	3.44	-1.1
J4	BC	2.60	-2.12
J5	BC	2.32	-2.16
J6	BC	2.1	-1.71
J7	T	2.97	-3.18
J8	T	1.64	-2.33
J9	T	2.19	-1.02

Appendix II. Data from IR-MS, each value is VPDB (permil) of each isotope in the rock sample. Localities: Baker's Cabin (BC), Belemnite Hill (BH), Poison Spider (PS), Greybull (G), Highway (H), and Thermopolis (T). Luminescent samples are not included in this table.

Appendix III

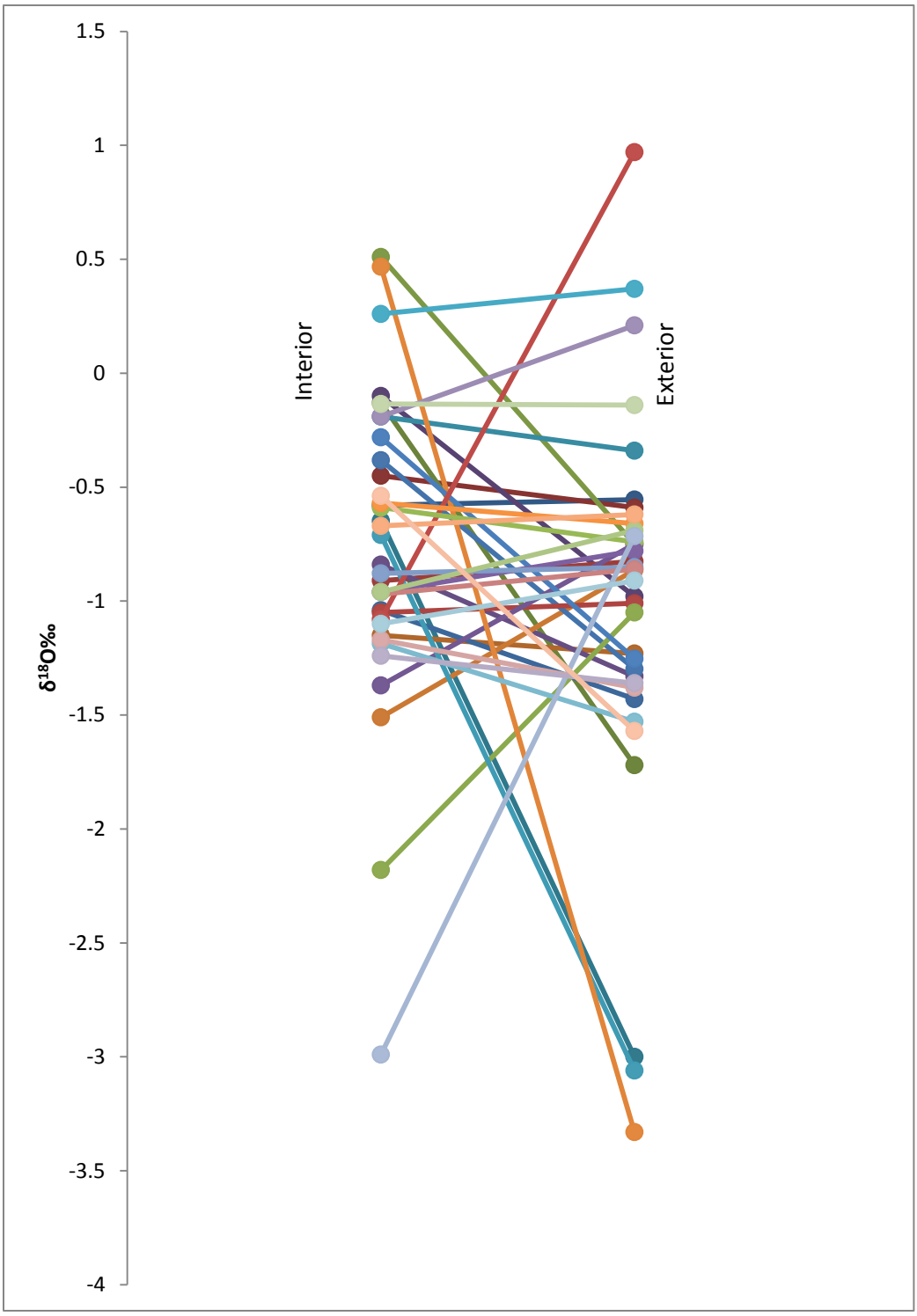

Appendix III. $\delta^{18}O‰$ of each sample plotted in relation to its pairing within a single belemnite. x-axis indicates where the sample was taken in relation to the center of the belemnite. Each line represents a single belemnite.

References

BARTLEY, J.K., SEMIKHATOV, M.A., KAUFMAN, A.J., KNOLL, A.H., POPE, M.C., and JACOBSEN, S.B., 2001, Global events across the Mesoproterozoic-Neoproterozoic boundary: C and Sr isotopic evidence from Siberia: Precambrian Research, v. 111, p. 165-202.

DERA, G., PUCEAT, E., PELLENARD, P., NEIGE, P., DELSATE, D., JOACHIMSKI, M. M., REISBERG, L. and MARTINEZ, M., 2009, Water mass exchange and variations in seawater temperature in the NW Tethys during the Early Jurassic; evidence from neodymium and oxygen isotopes of fish teeth and belemnites: Earth and Planetary Science Letters, v. 286, p. 198-207.

DOYLE, P. and BENNETT, R., 1995, Belemnites in biostratigraphy: Paleontology, v. 38, p. 815-829.

DUTTON, A., HUBER, B. T., LOHMANN, K. C. and ZINSMEISTER, W. J., 2007, High-resolution stable isotope profiles of a dimitobelid belemnite; implications for paleodepth habitat and late Maastrichtian climate seasonality: PALAIOS, v. 22, p. 642-650.

EREZ, J., and LUZ, B., 1983, Experimental paleotemperature equation for planktonic foramnifera: Geochimica et Cosmochimica Acta, v. 47, p. 1025-1031.

FRIEDMAN, I., and O'NEIL, J.R., 1977, Data of Geochemistry, Sixth Edition, Chapter KK. Compilation of stable isotope fractionation factors of geochemical interest. U.S. Geological Survey Professional Paper 440-KK, U.S. Government Printing Office, Washington.

GORE, P.J.W.: Jurassic history of North America, 2006, January 26, http://higheredbcs.wiley.com/legacy/college/levin/0471697435/chap_tut/chaps/chapter13-04.html. Checked March 2012.

GROSSMAN, E. L., 2012, Applying oxygen isotope paleothermometry in deep time, *in* Ivany, L., Huber, B., eds., Reconstructing Earth's Deep-Time Climate: Yale University Printing and Publishing Services, New Haven, p. 39-67.

HENDERSON, R.A. and PRICE, G.D., 2012, Paleoenvironment and paleoecology inferred from oxygen and carbon isotopes of subtropical mollusks from the late Cretaceous (Cenomanian) of Bathurst Island, Australia: PALAIOS, v. 27, p. 617-626.

IMLAY, R., 1947, Marine Jurassic of Black Hills area, South Dakota and Wyoming: Bulletin of the American Association of Petroleum Geologists, v. 31, p. 227-273.

IVANY, L.C. and RUNNEGAR, B., 2011, Early Permian seasonality from bivalve $\delta^{18}O$ and implications for the oxygen isotopic composition of seawater: Geology, v. 38, p. 1027-1030.

KIM, S.T., and O'NEIL, J.R., 1997, Equilibrium and nonequilibrium oxygen isotope effects in synthetic carbonates: Geochimica et Cosmochimica Acta, v. 61, p. 3461-3475.

KUEHN, S.: Geology of the Mesozoic Era: 245 to 66 million years ago, 2006, September 14, 2006, http://web.archive.org/web/20060914124516/http://geology.csustan.edu/kuehn/Geol2200/Mesozoic2_4.pdf. Checked March 2012.

O'NEILL, B.R., MANJER, W.L., and HAYS, P.D., 2003, Growth and diagenesis of middle Jurassic belemnite rostra from northeastern Utah: Insights using cathodoluminescence: Berliner paläobiologische Abhandlungen, v. 3, p. 241-251.

PEARSON, P.N., 2012, Oxygen Isotopes in foraminifera: Overview and historical review, *in* Ivany, L., Huber, B., eds., Reconstructing Earth's Deep-Time Climate: Yale University Printing and Publishing Services, New Haven, p. 1-38.

PLOYNOI, M., 2007, Development of Middle Jurassic microbial buildups in the Bighorn Basin of Northern Wyoming: Unpublished M.S. thesis, Wichita State University, Wichita, 98 p.

PRICE, G.D., TWITCHETT, R.J., SMALE, C., and MARKS, V., 2009, Isotopic analysis of the life history of the enigmatic squid *Spirula spirula*, with implications for studies of fossil cephalopods: PALAIOS, v. 24, p. 273-279.

REXFORT, A. and MUTTERLOSE, J., 2006, Stable isotope records from Sepia officinalis; a key to understanding the ecology of belemnites: Earth and Planetary Science Letters, v. 247, p. 212-221.

ROSALES, I., ROBLES, S., and QUESADA, S., 2004, Elemental and oxygen isotope composition of early Jurassic belemnites: Salinity vs. temperature signals: Journal of Sedimentary Research, v. 74, p. 342-354.

STANLEY, S., 2009, Earth System History: Clancy Marshall, New York, 551 p.

STEVENS, G.R. and CLAYTON, R.N., 1971, Oxygen isotope studies on Jurassic and Cretaceous belemnites from New Zealand and their biogeographic significance: New Zealand Journal of Geology and Geophysics, v. 14, p. 829-897.

TURNER, C. E. and PETERSON, F., 2004, Reconstruction of the Upper Jurassic Morrison Formation extinct ecosystem; a synthesis: Sedimentary Geology, v. 167, p. 309-355.

ULLMANN, C., WIECHERT, U. and KORTE, C., 2010, Oxygen isotope fluctuations in a modern North Sea oyster (Crassostrea gigas) compared with annual variations in sea water temperature; implications for palaeoclimate studies: Chemical Geology, v. 277, p. 160-166.

UNITED STATES GEOLOGIC SURVEY: Geological Survey Bulletin 1021-1: Geology of Devils Tower National Monument, Wyoming, 2005, updated March 1, 2005, http://www.nps.gov/history/history/online_books/deto/sec1.htm. Checked March 2012.

WIERZBOWSKI, H. and JOACHIMSKI, M. M., 2009, Stable isotopes, elemental distribution, and growth rings of belemnopsid belemnite rostra: Proxies for belemnite life habitat: PALAIOS, v. 24, p. 377-386.